Environ Sci Pollut Res (2013) 20:4711–4728
DOI 10.1007/s11356-012-1434-7

RESEARCH ARTICLE

The assessment of particulate matter emitted from stone-crushing industry by correlating rock textures with particles generated after comminution and dispersed in air environment

Girolamo Belardi · Gianluca Vignaroli · Paolo Plescia · Luciano Passeri

Received: 20 July 2012 / Accepted: 13 December 2012 / Published online: 5 January 2013

Abstract The generation and emission of particulate matter from abrasion industry are subjects of the pollution monitoring by multidisciplinary study involving earth sciences and engineering disciplines. This work investigates the correlation between textural properties of in situ rock with class size distribution and morphology of particles generated after rock comminution and particles emitted in the air. A special comminution-dust sampling architecture was realised. The combined use of scanning electron microscopy and particle size analyser was considered in performing digital image analysis on both crushed products and airborne particles collected onto membrane filters. The results show that the size and morphology of crushed particles are linked to the petrographic rock properties. In particular, particles with fibrous morphology are prominent in rocks showing foliated textures where elongated minerals occurred, with implication for asbestos-bearing rocks. For what concerns the airborne particles, the results show that their aerodynamic diameters are independent of the crusher operating conditions. External parameters probably intervene in the distribution of the airborne particles emission, including the dynamic air fluxes, or environmental conditions. By applying mathematical models, the morphology and size range of airborne particles following the comminution processes can be predicted, and results has implication for pollutants contamination due to particulate matters emitted by crush stone industry.

Keywords Airborne particles · Particulate matter · Comminution process · Rock petrographic texture · Environmental pollution · Crush stone industry

Responsible editor: Gerhard Lammel

G. Belardi · P. Plescia · L. Passeri
Istituto di Geologia Ambientale e Geoingegneria, Consiglio Nazionale delle Ricerche (CNR) Area della Ricerca di Roma RM1 Montelibretti, Via Salaria km. 29,300, 00016 Monterotondo, Rome, Italy

G. Vignaroli (✉)
Dipartimento di Scienze Geologiche,
Università degli Studi Roma Tre, L.go S.L. Murialdo,
1-00146 Rome, Italy
e-mail: vignarol@uniroma3.it

Introduction

The particulate matter (PM) emitted by the abrasion industry provides a considerable contribution of the total direct emission of fine particles suspended in the atmosphere (Evans 2005) and represents one of the major pollutants contaminating the air quality (US-EPA 2012). PM concentrations are continuously monitored in sites where excessive dust emissions are expected (e.g. all the industrial activities involving stone crushing), with proposition of informative guidelines and regulations on the potential danger due to the particulate emission (US-EPA 2012; Petavratzi et al. 2005). The negative environmental impact of fine particles suspended in the atmosphere is invariably connected with effects on the human health. Exposure to any dust in excessive amounts may cause harmful effects through inhalation, as well as by skin or eye contact and ingestion, depending upon the individual physical and chemical properties of dust (Health and Safety Executive 1997; World Health Organization 1999; Naidoo et al. 2002). For example, it has been documented that serious health concerns are directly connected with persistent inhalation of particles of silica component and fibrous morphology (e.g. Doll 1955; Rey et al. 1994; Cattaneo et al. 2006).

The normative evolution faces increasingly the issue of particulate emissions by industrial activities involving stone crushing, such as tunnelling, quarrying, and mining. European normative establishes the requirements for particulate emissions that the competent authorities should face, taking into

consideration the danger of dust, the mass flows, the emissions durability, the weather conditions and the general environment. For example, a large number of active quarries in Italy, addressed to a large variety of productions (e.g. railway ballast and roadbed, breakwater for protecting beaches or harbours, as well as ornamental stone), continuously faces international directives imposing a verification of modalities, quantities and morphological characteristics of generated dust, finalised to modulate the mitigation actions.

In mining industry, the production of PM is related to all the comminution operations of stones including primary crushing (by the means of jaw, impactor or gyratory crushers), secondary and tertiary crushing (by using cone crushers or other types of impactor crushers), screening and size classification. All of these operations can be significant sources of PM emissions if uncontrolled. Estimation of dust emissions from stone crushing process is mainly based on data and models proposed by the US-EPA (uses AP42: Compilation of air Pollutant Emission Factor). An emission factor is a representative value that relates the quantity of a pollutant released to the atmosphere with the industrial activity producing the pollutant. These factors for crushing operations are usually expressed as the weight of pollutant divided by a unit weight, volume, distance or duration of the activity. PM emission factors are in general calculated for PM30 (particles with aerodynamic diameter less than or equal to a nominal 30 μm), PM50, and PM100 by drawing an extrapolation line through the PM2.5 and PM10 (inhalable fraction), while few data are produced for the total suspended particles and relative morphology. Each of these particle sizes is used by regulatory agencies as the definition of upper limits of inhalable, thoracic and respirable fraction. The proposed emission factors can provide practitioners a useful tool for the quantification of emissions from industrial activities.

A number of recent researches has been devoted to the characterisation of airborne dust (e.g. Jones et al. 2002; Kissell 2003; DeCarlo et al. 2004; Reed 2005; Petavratzi et al. 2007; Zakrzewska et al. 2008), assessing the morphology of the airborne particles consistently depends on factors leading to the principal working phases (including the breaking method and the velocity of loading). However, it is worth noting that the emission of the airborne particles generated after rock comminution depend not only on the typology of the productive cycle but also on the aptitude of the starting material (the rock prototype) for fragmenting in smallest parties. As the PM is mainly composed by fragments of rock and rock-forming minerals, the source for dust hazard most commonly resides in the chemical composition and morphological characteristics of the starting material. For example, the processing of ophiolitic rocks (i.e. rock sequences with mafic and ultramafic composition) induces environmental impact due to production and dispersion of particles with fibrous habit and silica chemistry. These fibre-shaped particles are characterised by their large aspect (or length-to-width) ratio and small diameter (e.g. World Health Organization 1986; Gunter et al. 2007). The petrographic structure (massive or involved by anisotropic features, i.e. foliation) and the minero-chemical characteristics of the rock may be, then, considered as a first order parameter that control the size reduction process of rock. Understanding the existing relationships between the properties of the starting material, the particles generated after comminution, and the particles dispersed in atmosphere is a basic topic for discussing the environmental impact due to the stone crushing industry.

Adopting a multidisciplinary approach, this study deals with the size and the morphology of particles generated as a result of comminution through crushing of different types of rock, and particle available in air environment. We firstly describe the material properties in terms of minero-petrographic characteristics, highlighting the rock texture heterogeneities possibly producing fine grains. Then, we present the results (in terms of cumulative percentage, size and morphology) of both the experimental comminution process producing PM and simulation modelling for airborne dust. We investigate the correlation between rock textures, size reduction operating conditions and morphological characteristics of particles generated by crushing processes and dispersed in air environment. The obtained results provide concrete evaluation of the impact of stone-crushing process on the generation and emission of fine particles suspended in the atmosphere. The results have been used to propose a conceptual approach for the characterisation of particles generated after comminution of a rock and to develop appropriate mitigation strategies.

Description of the adopted procedure and methodologies

The rationale adopted for this work is simplified in the sketch of Fig. 1. For achieving the aims of the study, a multidisciplinary approach was considered, by integrating the insights coming from the observations on petrographic and mineralogical features on rock samples with an engineering study on rock crushing. The petrographic/mineralogical approach investigates the main material properties at different scale of observations. The engineering study focuses both on the experimental apparatus and the modelling of the phenomena. The main purpose of the engineering study is to define morphological aspects of two types of particles generated after comminution: (1) particles with size lower than 0.125 mm deposited at the ground and destined to waste and (2) particles dispersed in the atmosphere (that we called as airborne particles).

Characterisation of the rock samples

Firstly, we collected rock samples on the basis of the meso-scale properties. The spatial arrangement of the main

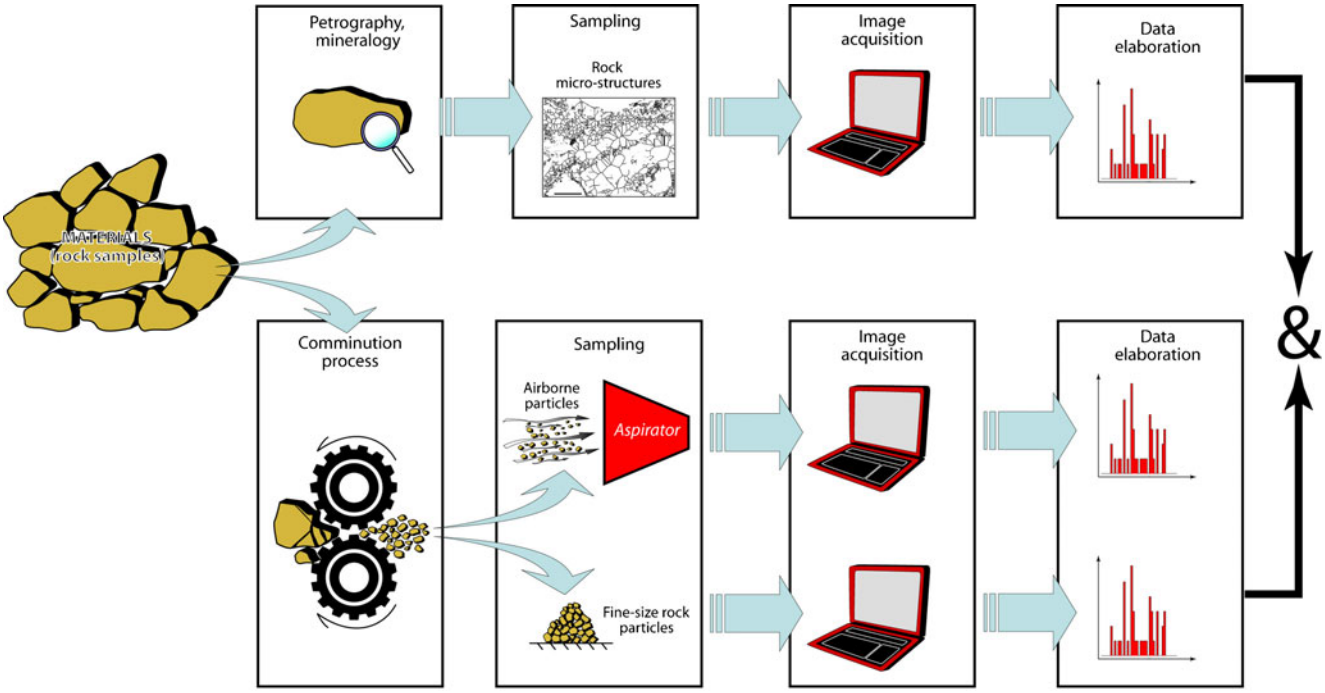

Fig. 1 Schematisation of the multidisciplinary methodology adopted in this study, integrating insights from rock petrographic analyses with stone crushing processing

constituent of the rock (i.e. the petrography texture), the chemical composition and the morphological habit of the minerals were the main rock features that have been studied in detail. Observations were performed on polished thin sections (30 μm thick) carried out from selected samples. Thin sections were obtained from sample cuts oriented both perpendicular and parallel to the major texture anisotropy (e.g. bedding and cleavage) unravelled at the meso-scale. Observations were firstly taken with an optical transmitted light microscopy (equipped with ×2.5, ×4, ×10, ×20 and ×40 magnifications and digital camera acquisition) and detailed by using a scanning electron microprobe (SEM;FEI Quanta 400 MK2 model) with operative conditions of 15 kV and point-beam 1–5 μm in size.

Digital images of thin sections were acquired by optical microscopy and processed with software Image-Pro Plus ver. 6.0, in order to produce a dot matrix data structure (raster images) (Fig. 2). To do this, after regulation of colour equalisation and contrast, the images were converted into a mosaic of traced objects. Each boundary between objects corresponds to real minero-petrographic features occurring at the thin section scale, i.e. mineral boundaries, mineral inclusions, micro-fractures and micro-veins, trace of foliation, etc. After that, the rasterised images were processed with counting tool, using the watershed split option provided by the software. The counting tool was mainly focused on the estimation of the longest and smallest caliper (Feret) lengths of each object. The ratio between major and minor

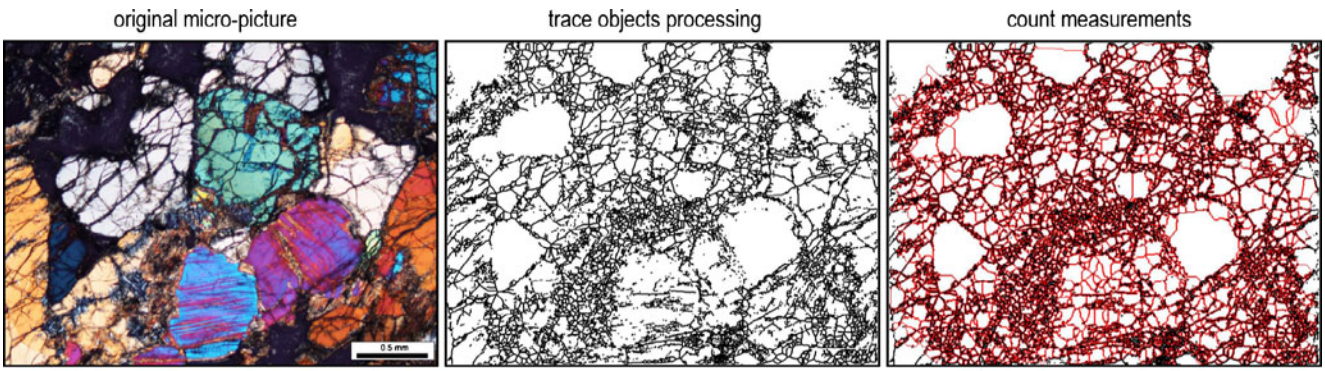

Fig. 2 Example of the digitalisation of optical microscopic images of thin sections for transposing the petrographic features into tracing objects and unraveling their geometric parameters

Feret diameters was considered as defining the aspect ratio of the object.

The comminution model

The average density of the samples was determined in accordance with the methodology laid down in technical standards UNI EN 1936:2001 using a hydrostatic balance AND (A&D Company Limited) GX600 model. The values of physical characteristics of the material were obtained by averaging the results of five determinations carried out on test pieces of different sizes.

Before crushing tests were performed, the samples were dried until average moisture below 1 % has been detected. Dried samples allowed to verify the production of dust at minimum opening jaws of the crusher.

Crushing tests were carried out by a jaw crusher model Retsch BB200. The primary operating variables in a jaw crusher are the open-side set (OSS) and closed-side set (CSS; linked from the throw) that determine the characteristic size of the product. OSS and CSS are the maximum and minimum distance of crusher jaws, respectively. Four CSS (of 5, 10, 15 and 20 mm) were tested for obtaining class size distributions of products that are consistent with those derived by the tertiary/quaternary crushing operation (e.g. Belardi and Desalvo 2006). For each CSS, a synthetic feed were used with a feed rate of about 400 $\mathrm{kg\,h^{-1}}$.

We adopted a mathematical model in order to simulate the laboratory crushing operation, on the base of the classification-breakage cyclic model (Whiten 1972, 1973; Whiten et al. 1973; Whiten and White 1979). The parameters in the classification-breakage functions can be estimated from the distributions of the measured particle size. Once established for a particular material in a determined crusher, these parameters remain independent to the OSS and CSS. The operation of a crusher is periodic with each period consisting of a nipping action and an opening action. During the nipping action, the jaw movement produces rock fragmentation by inducing a compressive stress on samples. The production of fine particles mainly derives from the chipping process, i.e., from rock fragmentation attaining at localised high pressure (e.g. King 2001; Liu et al. 2002) during grain–jaw and grain–grain hurts. During the opening action, part of the material moves downward into the crusher and some material falls through and out together with a certain amount of the fresh feed. This behaviour can be described quantitatively and modelled in terms of discrete size distributions. The model is based on the idea that progeny population is made up of a mixture of two separate populations that can be described by cumulative distribution as follows:

$$B_{ij} = k\left(\frac{D_i}{d_j}\right)^{n1} + (1-k)\left(\frac{D_i}{d_j}\right)^{n2}$$

Where:

- B_{ij} Cumulative weight of the material of size i that remains in size interval j after breakage
- d_j Initial size of the material
- D_j Biggest diameter of the material present in the size class after breakage
- $n1$, $n2$ Experimental data defining the slope of the B function for the fine and the coarse fraction, respectively (King 2001). It was assumed for n_1 the value of 0.5 and for n_2 the value of 4.5.

The first term in the equation above represents the size distribution of the fine fraction in the population of progeny particles and k is the fraction of daughter products that contribute to the finer fraction. The values of b_{ij} and b_{jj} are obtained from the cumulative breakage function by:

$$b_{ij} = B\left(D_{i-1},\ d_j\right) - \mathrm{B}\left(\mathrm{D_i}, \mathrm{d_j}\right);$$

$$b_{jj} = 1 - \mathrm{B}\left(\mathrm{D_j},\ \mathrm{d_j}\right)$$

and they represent the fraction of the material of size i or j that remains in the size interval j after breakage.

The model is valid for jaw and gyratory crushers that are used mostly for primary crushing and for cone crushers that are common for secondary, tertiary, and quaternary crushing duties.

Through this model, it is possible to simulate the distribution of sizes in the product from the knowledge of the classification and breakage function c_i and b_{ij} and the size distribution in the feed. We adopted the classification function proposed by Whiten (1972, 1973) and Whiten and White (1979):

$$C_i = 1 - \left(\frac{d_{pi} - d_2}{d_1 - d_2}\right)^2 \text{ for } \mathrm{d_1} < \mathrm{d_{pi}} > \mathrm{d_2};\ \mathrm{C_i} = 0 \text{ for } \mathrm{d_{pi}} \leq \mathrm{d_1}; \mathrm{C_i} = 1 \text{ for } \mathrm{d_{pi}} \leq \mathrm{d_2},$$

where d_1 is the smallest size particle that can be retained in the crushing zone during the opening phase of the cycle, and d_2 is the largest particle that can fall through the crushing zone during the opening phase of the cycle. Both parameters are characteristic of the crusher. Both d_1 and d_2 are assumed proportional to the OSS as follows:

$$d_1 = \alpha_1 * \mathrm{OSS}; \mathrm{d_2} = \alpha_2 * \mathrm{OSS}.$$

The values of the parameters α_1, α_2 and k were estimated from particle size distribution in the products from lab crushing tests by the software MODSIM ver. 3.4.0 (King 2001).

Characterisation of particles after comminution

Dry size analyses were carried out by ISO series sieves. The size distribution was obtained in wet mode by a laser

particle size analyser, model Sympatec Helos, equipped with He–Ne laser source. The morphological characterisation was performed on the fraction lower than 0.125 mm obtained by dry screening. The particle images were acquired with a camera mounted on a 1064L/LD CILAS particle size analyser and processed by software ExpertShape ver. 2.27. The geometrical parameters of particle that have been taken into consideration were the longest and smallest caliper (Feret) lengths, plus the area included in the polygon defining the particle outline. On the same polygon, the particle perimeter was estimated. The ratio between major and minor Feret diameters was considered as defining the aspect ratio of the particle.

The experimental assembly for airborne particles

A special dust sampling architecture was realised to collect the airborne particles in the crushing chamber near the source of dust generation during jaw operation. The particles were collected using pre-assembled filters of Omega Specialty Instrument Co. of 0.8 μm, and diameter of 25 mm using an isokinetic sampler model Digit ISO Zambelli at an aspiration rate of 1.0, 1.5, 2.5 and 8.5 l min^{-1}.

Characterisation of airborne particles

Digital images were acquired by SEM at ×1,000 magnitude. Digital images were processed with Image-Pro Plus software (v6.0). For airborne particles, the aerodynamic diameters were calculated on the basis of the average density reported in Table 1, omitting the Cunningham correction factor. The dynamic shape factor was obtained from the bibliography (Johnson et al. 1987; Dahneke 1973, 1979) as a function of the aspect ratio of the particles. The amount of particles with equivalent diameter lower than 0.5 μm (diminutive particles) was practically negligible in all tests.

Statistical analyses

The statistical analyses were performed by combining the results from the EasyFit Mathwave software (v5.4) and the Gaussian best fit statistics (Wise et al. 1985) implemented in the Daisy3 software (Salvini 2004). The statistic goodness-of-fit and the correlation between the values of the theoretical and experimental probability were verified through the Kolmogorov–Smirnov test (Chakravarti et al. 1967).

Materials

We used six different lithological groups of rock belonging to an ophiolite suite: serpentinite, basalt, lherzolite, gabbro, marble and metagabbro. This material was chosen because it covers a large range of rocks that are extensively processed by the stone crushing industry for the production of railway ballast and roadbed, or involved in engineering works such as tunnelling, as like as they can be used as ornamental stones. As these kinds of

Table 1 Sample characteristics

Sample	Lithology	Texture	Grain size at the thin section scale	Main minerals	Secondary minerals	Textural locus of fine grain minerals (possible source of fibrous particles)	Average density ($g cm^{-1}$)
AN	Serpentinite	Intensively foliated	Homogeneous and very fine to fine (0.010–0.100 mm)	Srp and Am	Cal and Chl	Srp along foliation; Am in post-foliation micro-veins	2.92
AQ	Basalt	Massive	Slightly homogeneous and very fine to fine (0.020–0.300 mm)	Pl, Px, Chl and Am	Prn, Ttn and Qtz	Chl, Px, Am in matrix; Pl laths	2.90
LH	Lherzolite	Massive	Homogeneous and medium to coarse (0.100–2 mm)	Ol, Px and Srp	Chl and Am	Srp in micro-veins; Srp, Chl in coronitic structures	2.97
ME	Gabbro	Massive	Homogeneous, medium to coarse (0.100–2 mm)	Px, Pl, Fsp and Am	Chl and clay minerals	Chl, Am in coronitic structures	2.93
MF	Marble	Foliated	Inhomogeneous and fine to coarse (0.010–2 mm)	Cal, Phl and Am	Ttn	Phl, Am along foliation; Am in flakes	2.88
TA	Metagabbro	Massive and slightly foliated	Inhomogeneous and very fine to coarse (0.010–2 mm)	Px, Pl, Am, Chl and Ep	Pmp, Ms and Qtz	Am, Chl, Pmp along foliation; Am, Chl in coronitic structures; Am, Pmp in micro-veins	2.96

Abbreviations: *Am* amphibole, *Cal* calcite, *Chl* chlorite, *Ep* epidote, *Fsp* feldspar, *Ol* olivine, *Phl* phlogopite, *Pl* plagioclase, *Pmp* pumpellyite, *Prn* prehnite, *Px* pyroxene, *Qtz* quartz, *Srp* serpentine, *Ttn* titanite

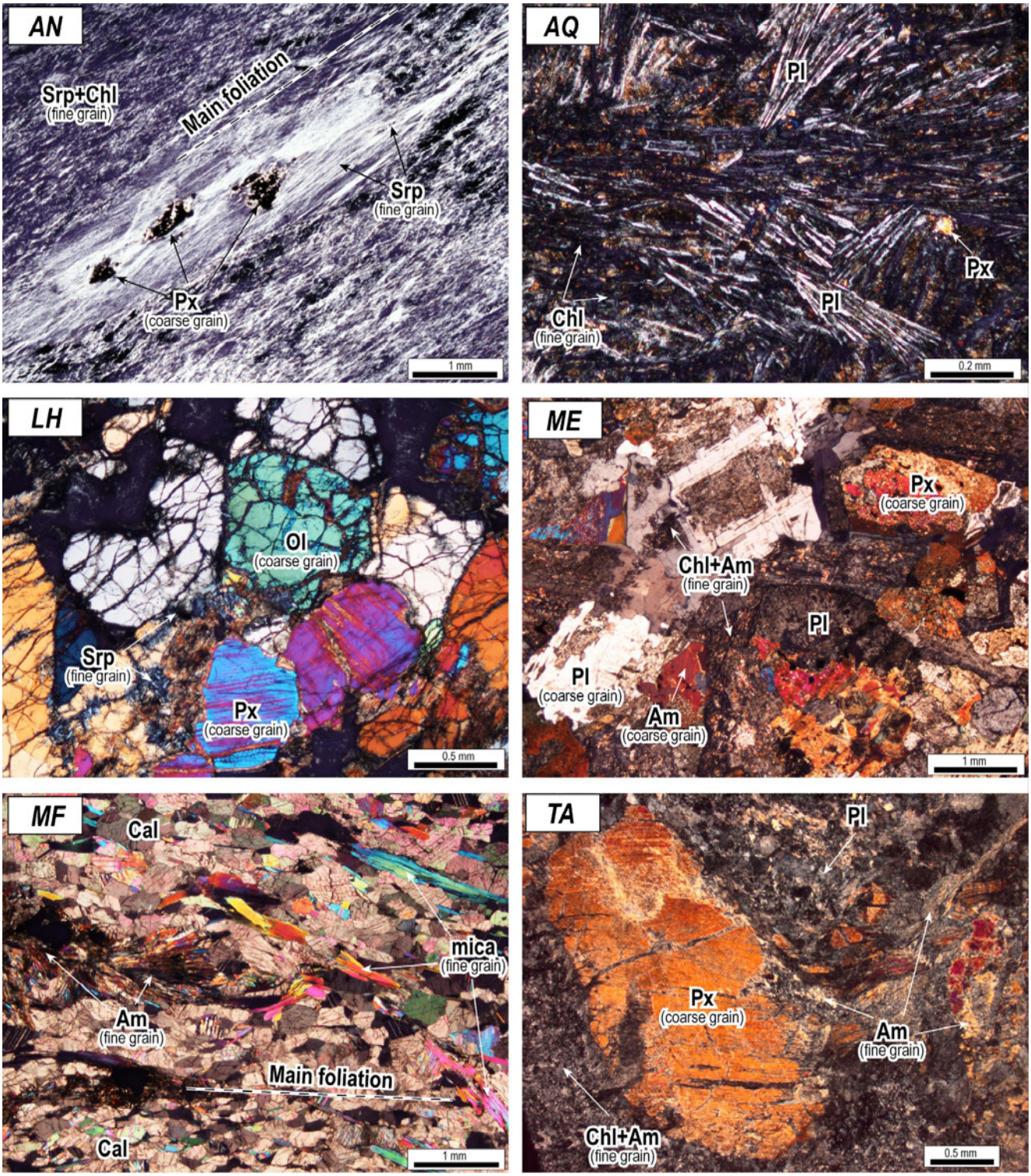

Fig. 3 Main petrographic features of the selected rock samples unraveled at the thin section scale. The micropictures show the textural differences between samples (i.e. a granular texture vs. foliated texture) and the grain size of the main minerals occurring

rock are commonly associated to environmental impact during excavation due to possible occurrence of asbestos minerals (e.g. Ross and Nolan 2003; Van Gosen 2007), i.e. serpentine- and amphibole-belonging minerals with length of >5 μm, width of <3 μm and aspect ratio of >3 (e.g. Gunter et al. 2007), they are frequently

subject of quality monitoring. The main properties of the considered samples area listed in Table 1.

Minero-petrographic characteristics

Sample AN—serpentinite

Samples are greenish and well foliated. Foliation thickness is sub-millimetric and large-size grains, up to 1 cm, occur within the foliation. At the thin section scale (Fig. 3), the petrographical texture shows evidence for a penetrative metamorphic assemblage that hosts few relicts of olivine, pyroxene, and plagioclase, as constituents of the pristine magmatic mineralogical association. The grains have irregular shape, often rounded. The diffuse metamorphic overprint consists of serpentine (mainly antigorite), chlorite, plagioclase, and amphibole. Serpentine and chlorite define the main foliation and grow with an elongated (lamellar and acicular) habit, with length not exceeding 200 μm.

Processing of digital images shows that a reduced number of objects that can be obtained. About 47 % of objects detected is at the mean aspect ratio (mean value, 2.30; standard deviation, 0.13) (Fig. 4).

Sample AQ-basalt

Samples show a dark grey colour, homogeneously diffused in the rock volume. The structure is massive, aphanitic, often cut by sub-millimetre veins. At the microscope (Fig. 3), the samples show variable textures characteristics, including vitrophyric, spherulitic, and intersertal, all identifying a low degree of crystallisation. The intersertal overgrowth of plagioclase laths is the dominant texture. Plagioclase laths are up to 300 μm in length and few microns in width. Plagioclase crystals show an elongated prismatic morphology. The interstices between plagioclase grains are occupied by glass or cryptocrystalline chlorite. Fine-grained pyroxene (diopside) and amphibole (Fe actinolite) can be observed as rounded, corroded crystals surrounded by plagioclase laths. Sets of micro-vein locally cut the texture. The occurrence of prehnite in veins suggests very low grade metamorphism for these samples.

A large number of objects were obtained from the processing of digital images. Objects characterised by the mean aspect ratio (mean value, 2.07; standard deviation, 0.10) are about 46 % of all features detected (Fig. 4).

Sample LH-lherzolite

Samples show a dominant dark green colour, with massive structure consisting of fine-grained matrix and porphyric olivine crystals. At the thin section scale (Fig. 3), the texture is isotropic, massive without evidence for foliation development. The main mineralogical association consists of olivine (forsterite), clinopyroxene (augite) and orthopyroxene (enstatite), all showing idiomorphic habitus. Grain size is dominantly homogeneous, medium-to-coarse grained. Sharp boundaries between minerals and 120° angles have been observed, documenting for a textural equilibrium during crystallisation. This texture is overprinted by secondary structures consisting of a microfracture network. Microfractures dissect olivine and pyroxene crystals with an anastomosed pattern. Microfractures are filled by fine grained serpentine (antigorite) crystals. It has been observed that the antigorite crystals are mainly disposed orthogonal to the wall fractures. Antigorite, and subordinated chlorite, also grows as very thin films around olivine and pyroxene grains (coronitic structures). Morphologically, olivine and pyroxene have rounded-to-tabular regular shape, whereas antigorite crystals are thin and elongated (acicular habit).

A reduced number of objects were obtained from the processing of digital images. The mean value of the aspect ratio is 2.07 (standard deviation, 0.10). Objects around the mean aspect ratio are about 43 % of all features detected (Fig. 4).

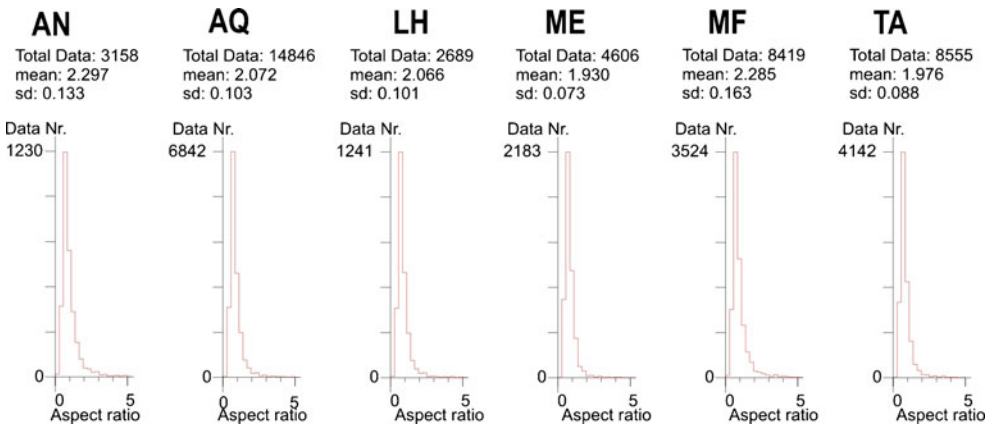

Fig. 4 Histograms showing the frequency of the aspect ratio as deduced from the rasterised images

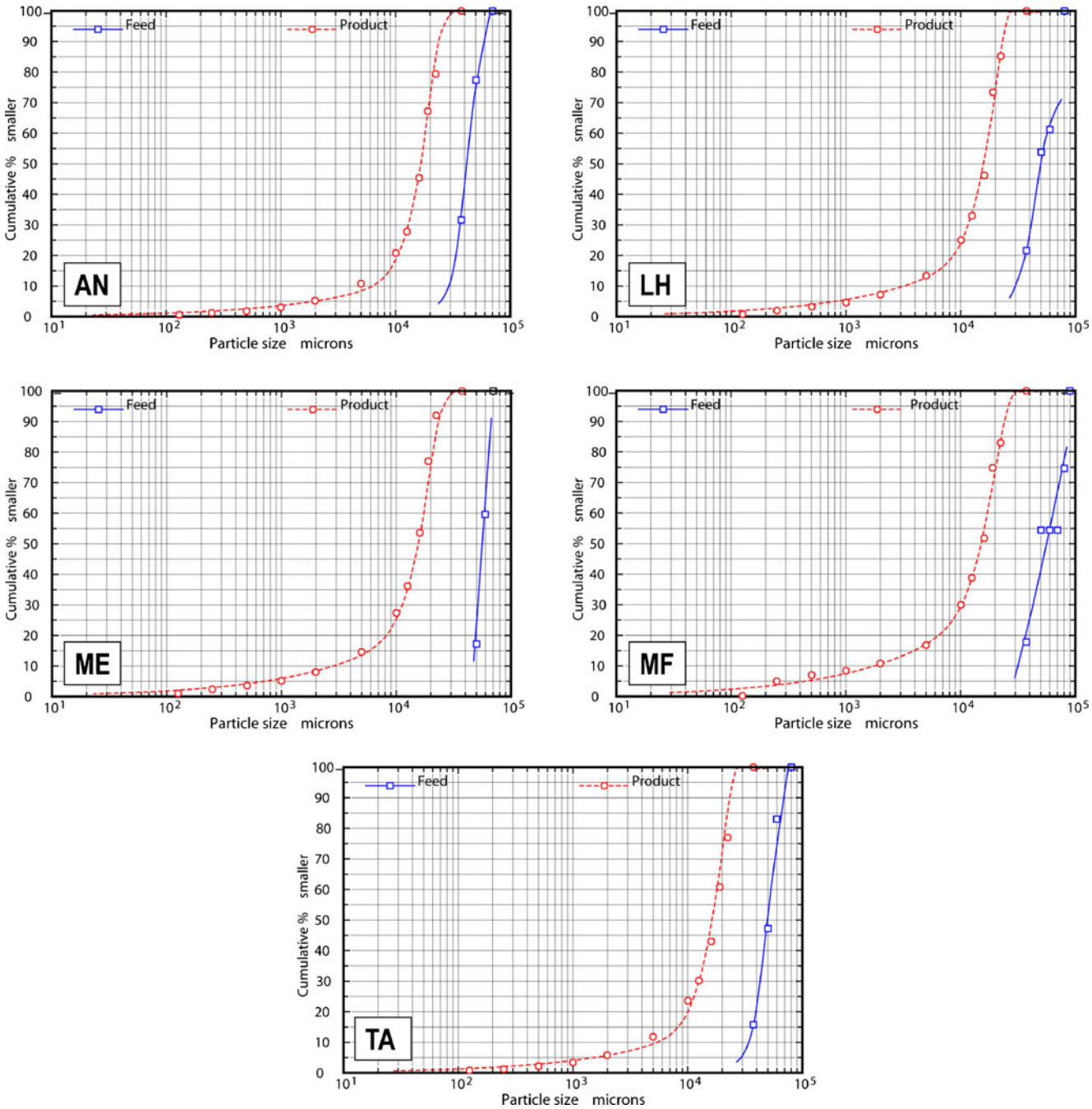

Fig. 5 Simulation results for a crusher closed side setting of 15 mm

Sample ME—gabbro

Samples are characterised by a dark green colour with sporadic whitish domains. The structure is massive, homogeneous, and homeogranular. The microscale texture (Fig. 3) mainly consists of large grains of pyroxene (augite), euhedral plagioclase (Ca rich) and feldspar (orthoclase). Crystals are randomly disposed, without any evidence of preferential structures of crystallisation (i.e. foliation). Sharp boundaries between crystals and crystallographic features document a magmatic nature for this petrographical texture. Evidence of chemical alteration and re-crystallisation has been observed. Feldspar shows alteration by the mean of clay minerals. Pyroxene is often rimmed (coronitic structures) by fine-grains of chlorite and green amphibole (Ca-rich). The latter also grows, together with Na-plagioclase, as constituent of micro-veins cutting through the magmatic assemblage. All detected minerals show a regular tabular-to-prismatic morphology (Fig. 4).

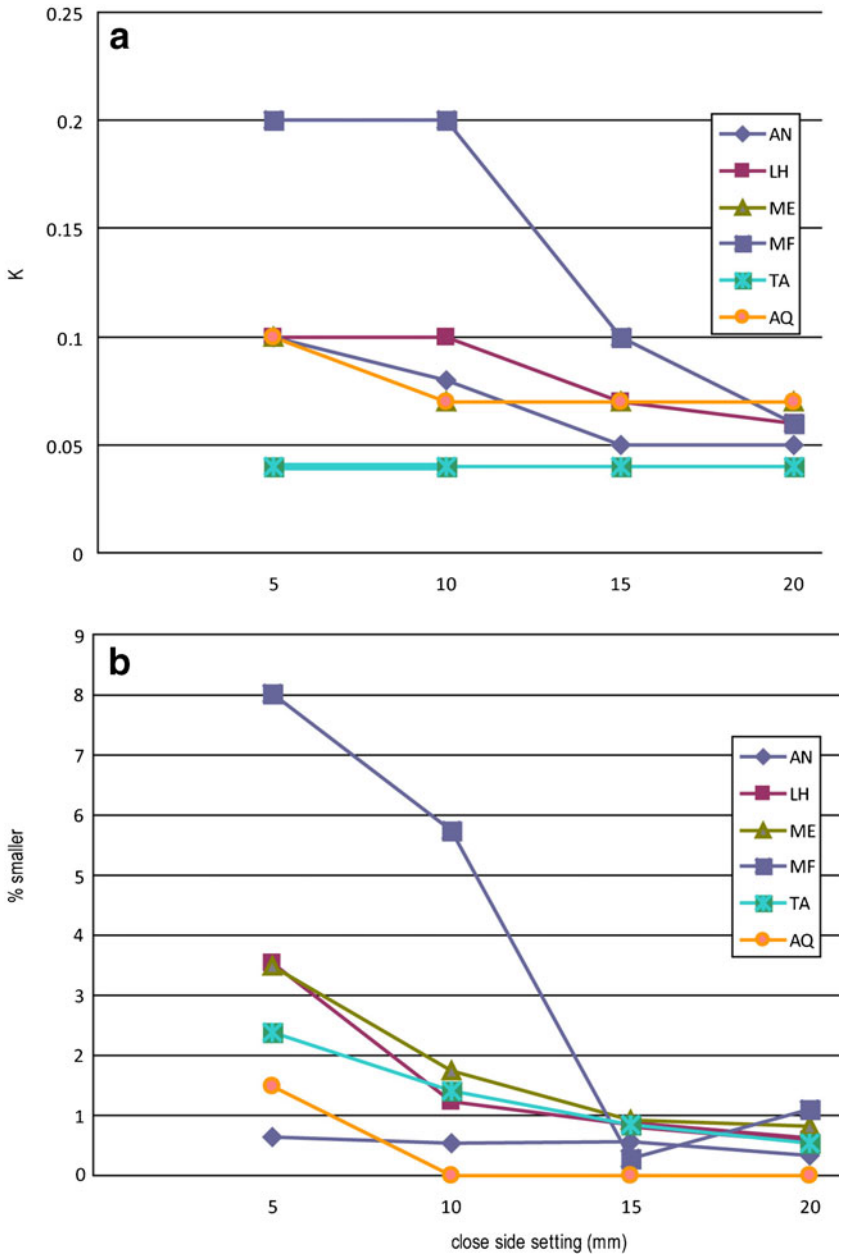

Fig. 6 **a** Simulation results for k parameter value; **b** percentage of crushed product with size lower than 0.125 mm

The processing of digital images provided a medium number of objects, characterised by a mean aspect ratio of 1.93 (standard deviation, 0.07). Objects around the mean aspect ratio are about 47 % of the amount (Fig. 4).

Sample MF—marble

Samples have a white-to-beige uniform colour and the structure is dominantly foliated. The grain-size is almost homogeneous, except for few elongated crystals disposed along the foliation. At the thin section scale (Fig. 3), the composite micro-texture consists of: (1) a granular, massive matrix of calcite crystals randomly disposed, with dimension not exceeding 300 μm and (3) a sub-millimetric foliation defined by the elongation of mica (phlogopite) and green amphibole (tremolite) crystals. Both amphibole and mica crystals show dimension up to 2 mm. Amphibole grows also in flakes, with radial disposition and showing a prismatic-to-acicular morphology.

The processing of digital images provided a medium number of objects, characterised by a mean aspect ratio of 2.29 (standard deviation, 0.16). Objects around the mean aspect ratio are about 42 % of the amount (Fig. 4).

Sample TA—metagabbro

At the meso-scale, the selected samples show an inhomogeneous colour made of cm-thick alternation of green-to-bluish levels and white levels. The structure is weakly foliated, with sporadic massive domains. The micro-texture is polyfasic (Fig. 3), as a magmatic assemblage is replaced by a metamorphic one, producing a heterogeneous grain-size. The magmatic structure consists of large pyroxene (augite) and plagioclase (albite-to-oligoclase) showing a tabular morphology. Pyroxene also shows evidence for brittle deformation due to the occurrence of micro-fracture systems. The metamorphic assemblage grows (1) in rim structures around the pyroxene, (2) within interstitial spaces between pyroxene and plagioclase, (3) along the incipient foliation and (4) in micro-veins cutting through the pristine assemblage. The metamorphic assemblage mainly consists of green amphibole (actinolite), albite, epidote, chlorite and pumpellyite. A prismatic-to-acicular habit has been observed for amphibole occurring within the matrix and along the metamorphic foliation, whereas fibrous morphology can be often detected in micro-veins.

The processing of digital images provided a medium number of objects, characterised by a mean aspect ratio of 1.98 (standard deviation, 0.09). Objects around the mean aspect ratio are about 48 % of the amount (Fig. 4).

Table 2 Probability density function of the laser size distribution of the material under 0.125 mm in the jaw crusher products

$$f(x) = \frac{\alpha}{\beta} * \left(\frac{\alpha}{\beta}\right)^{\alpha-1} * \exp\left(-\frac{x}{\beta}\right)^{\alpha}$$

Parameter	Closed side setting			
	5 mm	10 mm	15 mm	20 mm
Sample AN				
α	1.0581	1.0163	1.0236	1.0212
β	29.597	35.716	30.4460	30.1700
Mean diameter (μm)	28.946	35.478	30.155	29.91
Sample AQ				
α	1.0809	1.0112	1.1080	1.0919
β	55.595	56.355	58.455	57.499
Mean diameter (μm)	53.962	55.234	56.554	56.987
Sample LH				
α	1.014	1.0174	1.0625	1.0699
β	33.349	31.478	36.791	36.965
Mean diameter (μm)	33.157	31.254	35.928	36.009
Sample ME				
α	1.0917	1.0786	1.0385	1.0544
β	36.434	33.735	33.677	34.243
Mean diameter (μm)	35.245	32.769	33.169	33.534
Sample MF				
α	1.2351	1.2532	1.1419	1.25
β	63.028	51.923	70.783	62.757
Mean diameter (μm)	58.867	48.332	67.504	58.451
Sample TA				
α	0.94	0.92	0.95	0.91
β	29.49	31.49	33.12	31.70
Mean diameter (μm)	33.11	30.40	32.84	33.92

Experimental results and comments

Particles generated after comminution

The values of the parameters as obtained from the model simulation results are: α_1=0.3, α_2=1.3 for all materials and openings of the jaw crusher tested, while the parameter K was variable and depending on the opening of the crusher. The model fits the experimental data for all tested materials at CSS of 15 mm (Fig. 5). The parameter K, which is related to the quantity of the fine-size product, shows a decreasing trend with increasing the CSS (Fig. 6a). This decreasing trend has been not observed for TA sample, for which the parameter K remains constant at 0.04. As expected, with increasing the CSS, the percentage of particles with size

Table 3 Probability density function of the aspect ratio of the particles less than 0.125 mm present in the jaw crusher products

$$f(x) = \frac{\exp\left(-\frac{1}{2} * \left(\frac{\ln(x-\gamma)-\mu}{\sigma}\right)^2\right)}{(x-\gamma)*\sigma*\sqrt{2\pi}} \mathrm{X} \geq 1 \ \gamma = 1$$

Parameter	Closed side setting			
	5 mm	10 mm	15 mm	20 mm
Sample AN ($\sigma_{medio} = 0.72115 \mu_{medio} = -0.6810$)				
σ	0.99468	0.96515	0.97259	0.71916
μ	−0.50814	−0.49198	−0.48981	−0.73633
Sample AQ ($\sigma_{medio} = 0.689045$ $\mu_{medio} = -0.9615$)				
σ	0.68153	0.69781	0.70561	0.67123
μ	−0.95344	−0.96453	−0.95456	−0.97345
Sample LH ($\sigma_{medio} = 0.68965$ $\mu_{medio} = -084079$)				
σ	0.73099	0.69226	0.65826	0.6917
μ	−0.79794	−0.83256	−0.84071	−0.88836
Sample ME ($\sigma_{medio} = 0.67657$ $\mu_{medio} = -0.84363$)				
σ	0.65192	0.66555	0.6805	0.68121
μ	−0.86392	−0.79578	−0.83791	−0.89682
Sample MF ($\sigma_{medio} = 0.75447$ $\mu_{medio} = -0.79475$)				
σ	0.77947	0.78782	0.76873	0.71334
μ	−0.78499	−0.78461	−0.79155	−0.8111
Sample TA ($\sigma_{medio} = 0.76236$ $\mu_{medio} = -0.34737$)				
σ	0.75439	0.77236	0.50966	0.86384
μ	−0.4038	−0.29028	−1.5742	−0.76138

lower than 0.125 mm decreases lower than 1 % (Fig. 6b). Through the model adopted, it is possible to simulate the size distribution of product by considering the classification-breakage cyclic model and the feed size distribution.

The Weibull probability density function was chosen for modelling the frequency distribution of particles with size lower than 0.125 mm. The distribution parameters obtained from the calculations are reported in Table 2. Substantially, we note that a rather constant value of the mean diameter was obtained for each sample, independently of the minimum opening jaws of the crusher. These trends let to suppose that the frequency distribution does not depend on the experimental conditions, but it is more likely connected with the intrinsic properties of material (e.g. mechanical and textural characteristics).

The results of the statistical analysis of the particles aspect ratio are shown in Table 3 and the graphical outputs for some of the material tested are reported in Fig. 7. The results show that morphological spectrum of the generated particles is almost regardless of the opening jaws set adopted in the test. For all materials analysed the results shown that about 85 % particles has aspect ratio of ≤2 (which is indicative of a prismatic morphology), while particles with aspect ratio of ≥3 (acicular-to-fibrous morphology) constitute the tails of the frequency distribution. The average values of the frequency distribution allow determining the percentage of particles with a prefixed value of aspect ratio compared with the total generated particles.

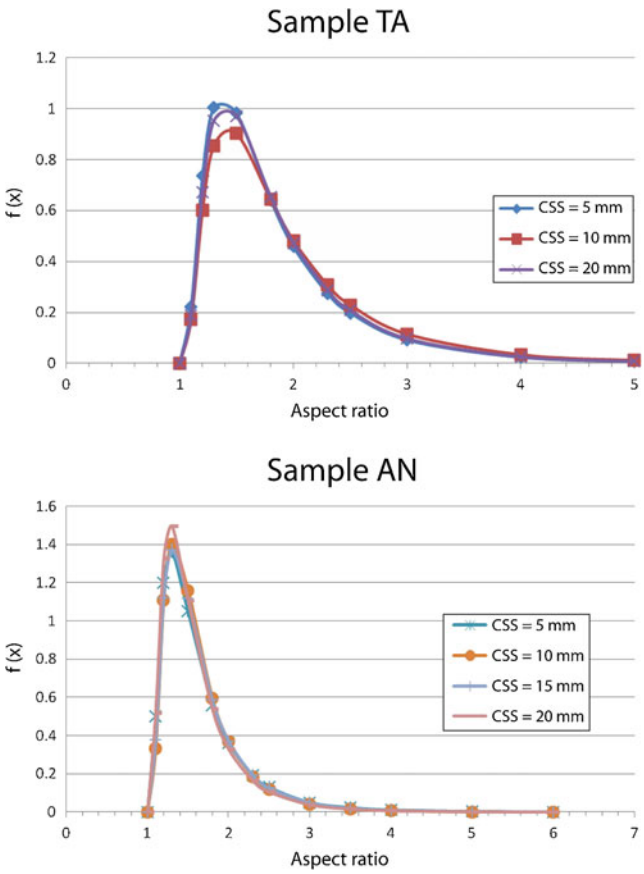

Fig. 7 Morphological distribution of the particles with size lower than 0.125 mm present in the jaw crusher product (samples AN and TA used as tests)

Figure 8 reports the histograms related to the distribution of the aspect ratio estimated for the crushed product with size lower than 0.125 mm (overall data obtained at the different CSS). The histograms refer both to the total of particles analysed and filtered particles having aspect ratio higher than 3.

Airborne particles

The probability density functions of the aerodynamic diameters (limited to 100 μm in length) of the particles present in the crushed product (size lower than 0.125 mm) are reported in Fig. 9. The coefficients of the log-normal distribution function are also reported. The diagrams show that the aerodynamic diameter distribution is almost independent from the CSS of the crusher. In order to verify the effect of aspiration rate on the size and shape of the airborne particles, some tests were carried out using the sample TA, by considering jaw CSS of 5 mm and aspiration rate of 1, 1.5, 2.5 and 8.5 $1m^{-1}$. The morphologic spectra of collected particles are shown in Fig. 10 while Table 4 shows the log-normal probability density function of the particles aspect ratio sampled at different aspiration rates. The mean aspect ratio deduced from the morphological spectra results to be nearly constant for the different aspiration rate tests. Moreover, the distribution of the aerodynamic diameter results to be independent on the aspiration rates. These insights let to image that the aspiration rate influences the amount of particles collected but not their morphological distribution.

The tests were carried out at various jaw closed side setting with an aspiration rate fixed at the value of 1.5 l min^{-1}. This aspiration rate was considered as optimal for avoiding the filters overload and assuring an objective analysis of the particulate. Figure 11 reports the probability distribution functions for particles with aspect ratio of ≤3 and for particles of aspect ratio of >3 unravelled from tests carried out on the sample AN and considering the CSS of 10, 15 and 20 mm. The results show that the morphological distribution of particles in the crushed material is almost independent of the opening of the crusher jaws. The trend of the probability density functions shows that the morphological distribution of the particles collected on filters is similar to that of particles in the crushed material. In case of occurrence of particles with fibrous shape, the airborne particles show a morphological distribution shifted towards lower values of aspect ratio, for all materials and closed side setting tested. This is probably due to the fact that the particles with fibre-like shape are hardly held in suspension. As a result, the amount of fibre-shape particles present in air environment is levelled independently by the type of crushed material.

Figure 12 illustrates the distributions of the aerodynamic diameters of the airborne particles as a function of the operating conditions of the crusher. The estimated average parameters of

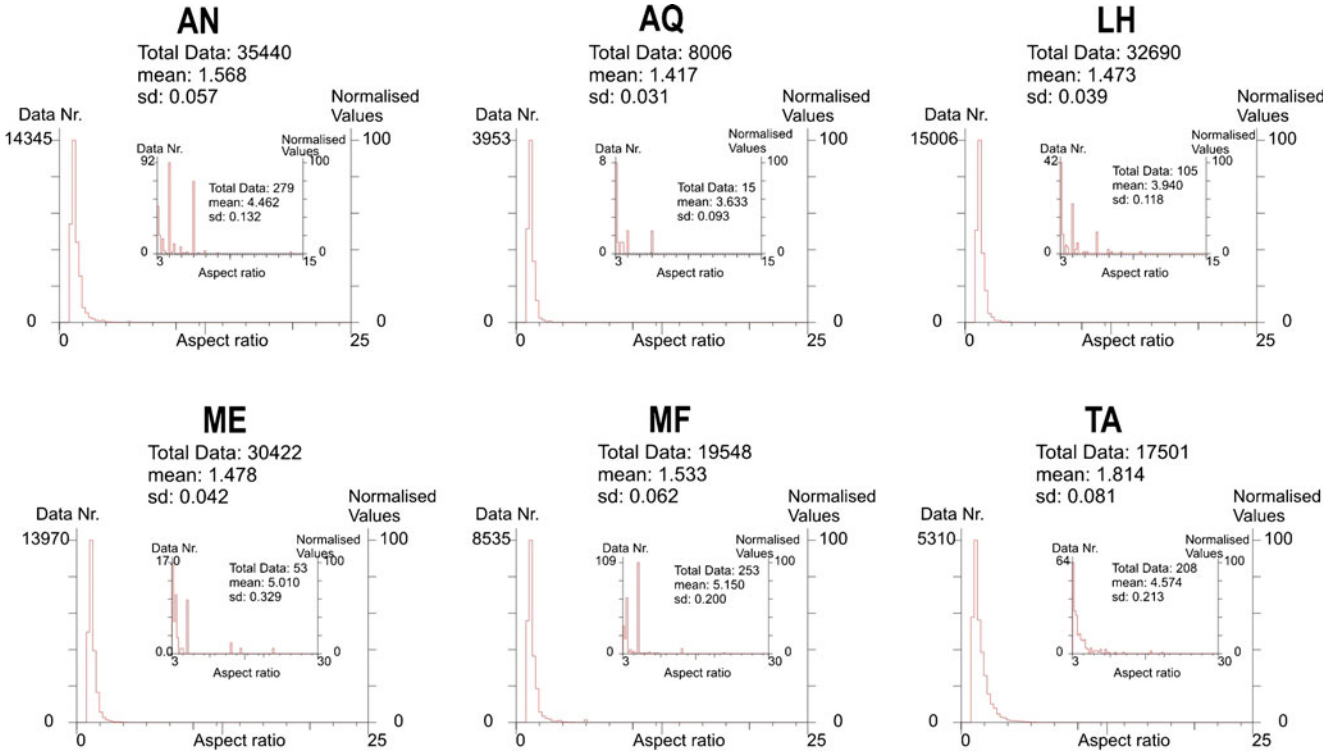

Fig. 8 Histograms showing the aspect ratio distribution of crushed product lower than 0.125 mm. Small histograms refer to aspect ratio for filtered particles having fibre morphology

the log-normal probability density functions are also reported. For each tested sample, the distributions show a maximum aerodynamic diameter of about 70–80 μm, which are independent from the crusher operating conditions. The mode and mean of the distributions resulted to be variable between 3 and 5 μm, and between 5 and 7 μm, respectively.

The resulted aerodynamic diameters of airborne particles is systematically lower than the upper limit of the aerodynamic diameter calculated for particles with size lower than 0.125 mm (occurring in the crushed product). Consequently, the distribution of the aerodynamic diameter of the particles lower than 0.125 mm can be used to predict also the aerodynamic diameter distribution of the particles released from the material and available in air environment.

Figure 13 reports the histograms related to the distribution of the aspect ratio estimated for the airborne particles. The histograms refer both to the total of particles analysed and filtered particles having aspect ratio higher than 3.

Discussion

The obtained results contribute to evaluate how the stone crushing process supply the generation and emission of fine particles suspended in the atmosphere.

From the rock texture to the airborne particles

The measurement of the emitted PM in mining operations is a required evaluation for defining the correct dust assessment and improving mitigation methodologies and safety regulations. Previous works demonstrate that a reduction of the dustiness during abrasion of natural stones can be achieved by optimising the sample mass and the time scale in industrial processes (Breum 1999; Petavratzi et al. 2007). Our results allow to try a correspondence between rock properties (in terms of rock structures and rock-forming minerals), particles generated after comminution processes and particles available in air environment.

Minero-petrographic investigations outline that the structures of the rock is related to the heterogeneities in the volume. These heterogeneities are defined by the variability of mineral shape (prismatic, rounded and fibrous) and the occurrence of peculiar structures (e.g. the foliation). Genesis of rock textures and shape of the minerals are two aspects intimately connected and they are expected to be the parameters controlling the formation of some PM, as in the case of the particles of asbestos (e.g. Vignaroli et al. 2011). In our cases, the different rock types show heterogeneities at the thin section scale that can be preliminarily expressed in terms of occurrence or absence of planar anisotropic features. In this case, we can distinguish between samples dominated by pervasive foliation (samples AN and MF)

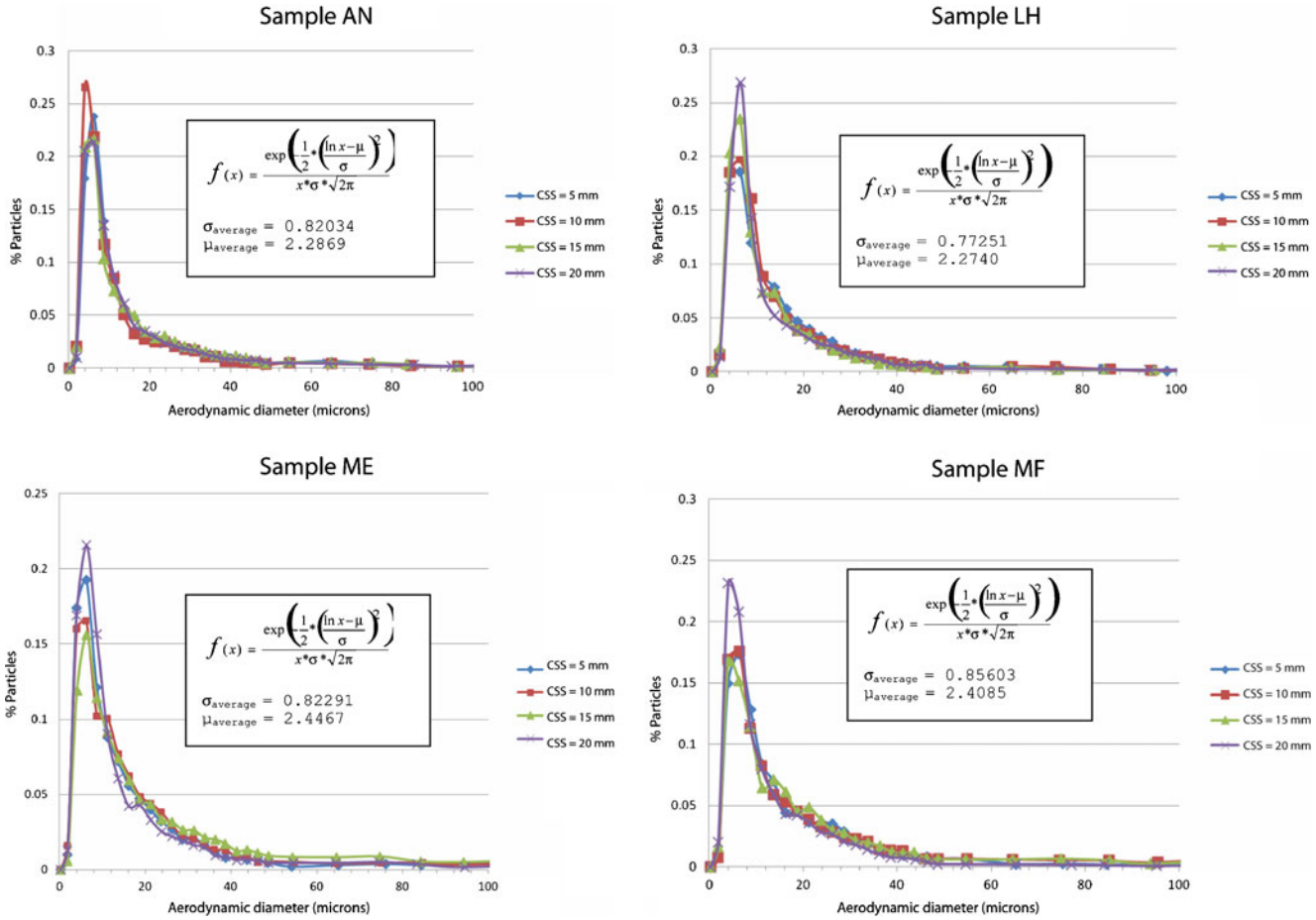

Fig. 9 Aerodynamic diameter distribution of the particles with size lower than 0.125 mm present in the jaw crusher product for the samples AN, LH, ME and MF

and samples with massive structures (samples AQ, LH, ME, and TA). At a first impression, it is intuitive to consider that an inhomogeneous structure may produce fragmentation more easily than a massive one. If we describe the rock structures by considering the aspect ratio of the rasterised objects, we can distinguish between low, medium, and high mean aspect ratio. Samples with low aspect ratio (ME and TA) are characterised by dominant coarse grain minerals, partly replaced by fine grain ones. A granular texture is prevalent in these samples, and the occurrence of structural heterogeneities (e.g. foliation) is subordinately. Conversely, samples with high aspect ratio (AN and MF) show the occurrence of minerals with high asymmetric habitus (acicular to fibrous). Noteworthy feature of these samples is the millimetric and sub-millimetric thick foliation that constitutes the rock micro-structure, along which the minerals are disposed. Medium values of aspect ratio for samples LH and AQ can be tentatively associated with a mixing of two components: the occurrence of a granular texture (i.e. without the development of foliation) and the crystallisation of fine grained minerals in specific micro-textural sites (e.g. the serpentinite in micro-veins).

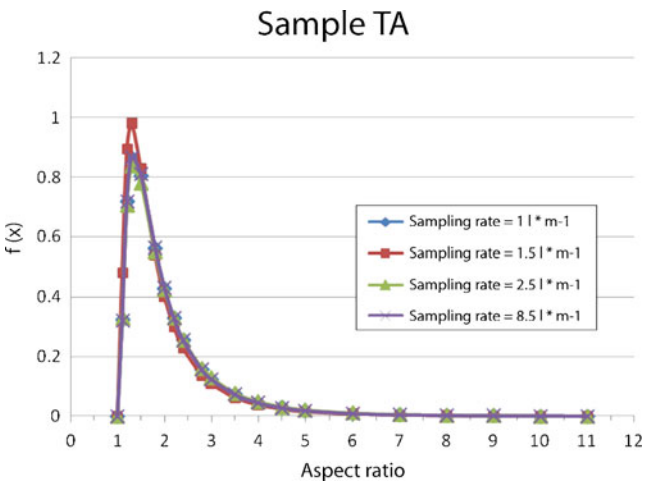

Fig.10 Morphological spectrum of the airborne particles as a function of aspiration rate (test with jaw closed side setting of 5 mm)

In Fig. 14, we present a correlation between aspect ratio distribution deduced from rasterised images with aspect ratio distribution of particles from comminution (with size lower than 0.125 mm) and airborne particles. To do this, we assume that the production of fine particles mainly derives

Table 4 Probability density function of the particles aspect ratio sampled at various aspiration rate (test with jaw closed side setting of 5 mm)

Parameters $(f(x) = \frac{\exp\left(-\frac{1}{2}*\left(\frac{\ln(x-\gamma)-\mu}{\sigma}\right)^2\right)}{(x-\gamma)*\sigma*\sqrt{2\pi}}$ $x \geq 1\gamma = 1)$	Sampling rates			
	1 l min^{-1}	1.5 l min^{-1}	2.5 l min^{-1}	8.5 l min^{-1}
Σ	0.89	0.90	0.90	0.88
μ	−0.27	−0.24	−0.25	−0.27

from the chipping process, i.e. from rock fragmentation attaining at localised high pressure during grain-jaw and grain-grain hurts. Chipping is a typical microscale process, which allows us to correlate with the microtexture properties. Even though preliminary, this correlation suggests that the size and morphology of crushed particles are in some way linked to the petrographic rock properties. One can expect that rocks dominated by pervasive foliation can easily produce elongated particles than massive rock, when crushed. The textural loci of fine grain minerals (as reported in Table 1) may be effectively the possible sources for fibrous particles.

An experimental approach

The size and morphology distribution and quantity of fine (lower than 0.125 mm) of the output material from the comminution process (jaw crusher, cone, gyratory and roll mill) can be modelled through the Weibull frequency distribution function by imposing the average value of 1.07 for the parameter α and the value varying from 30 to 60 μm for the β parameter. The resulting morphological spectrum of the generated particle is composed by a large part of the particle amount with aspect ratio of ≤2 (prismatic morphology), and the tail of the frequency distribution shows particles with aspect ratio of ≥3 (acicular-to-fibrous morphology). The test samples showed that the concentration of fine material may differ between different rock samples, but the mean diameter estimated was roughly independent of the minimum opening jaws of the crusher.

For what concerns the airborne particles, the results show that their aerodynamic diameters are independent of the crusher operating conditions. This suggests that the morphologic spectrum of airborne particles is quite similar to that of particles generated after the crushing process regardless of the closed side setting. These results should be compared with conclusions by Petavratzi et al. (2007) on limestone tests, as the authors documented that the size distributions of the particulates does not substantial change with respect the concentrations of fine material in the test samples.

To summarise, both distributions (particles lower than 0.125 mm of the crushed material and airborne particles) can be described by a log-normal probability density function independently from the operating conditions of the comminution machine. The morphological distribution of airborne particles was also independent of both the aspiration rate and opening of the crusher jaws. Only the amount of fine material (lower than 0.125 mm) depends on the crusher operating conditions. Thus, for the tested materials, it is therefore sufficient to characterise the particle fraction lower than 0.125 mm in the crushed material for estimating the size and shape distribution of particles available in air

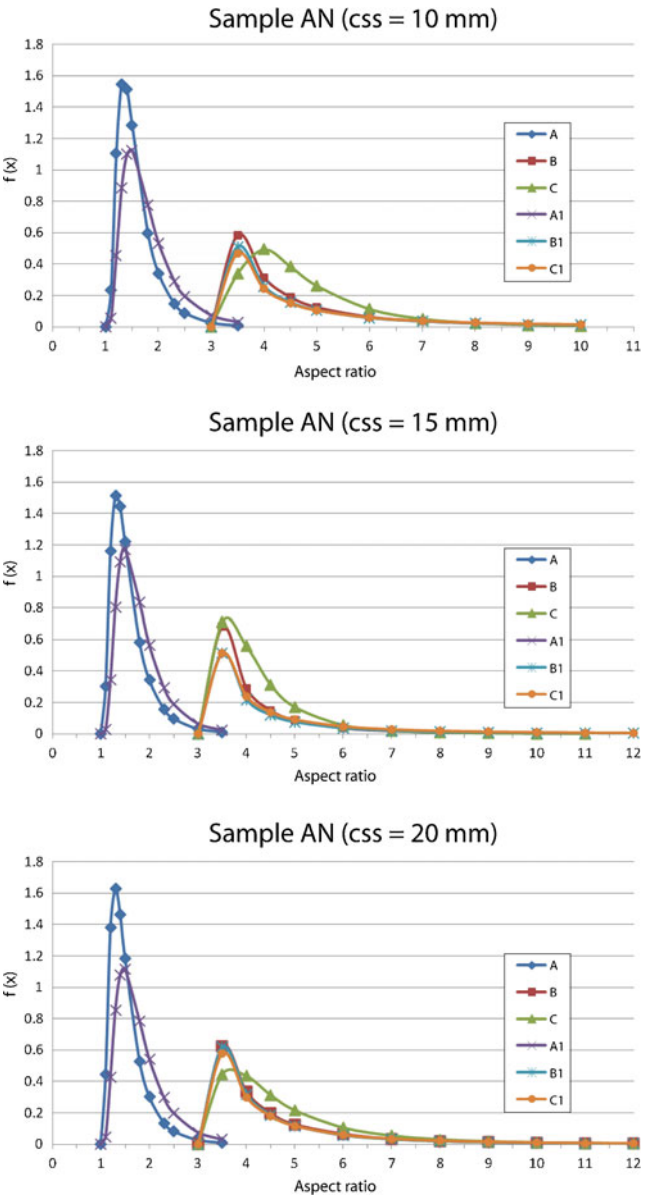

Fig. 11 Aspect ratio distribution for airborne particles and particle with size lower than 0.125 mm at aspiration rate of 1.5 l min^{-1} and different CSS for sample AN (used as test). Legend: *A* aspect ratio of <3 distribution in the crushed product, *A1* aspect ratio of <3 distribution in the airborne particles population, *B* aspect ratio of >3 distribution in the crushed product, *B1* aspect ratio of >3 distribution in the airborne particles population, *C* distribution in the crushed product, *C1* fibre distribution in the airborne particles population

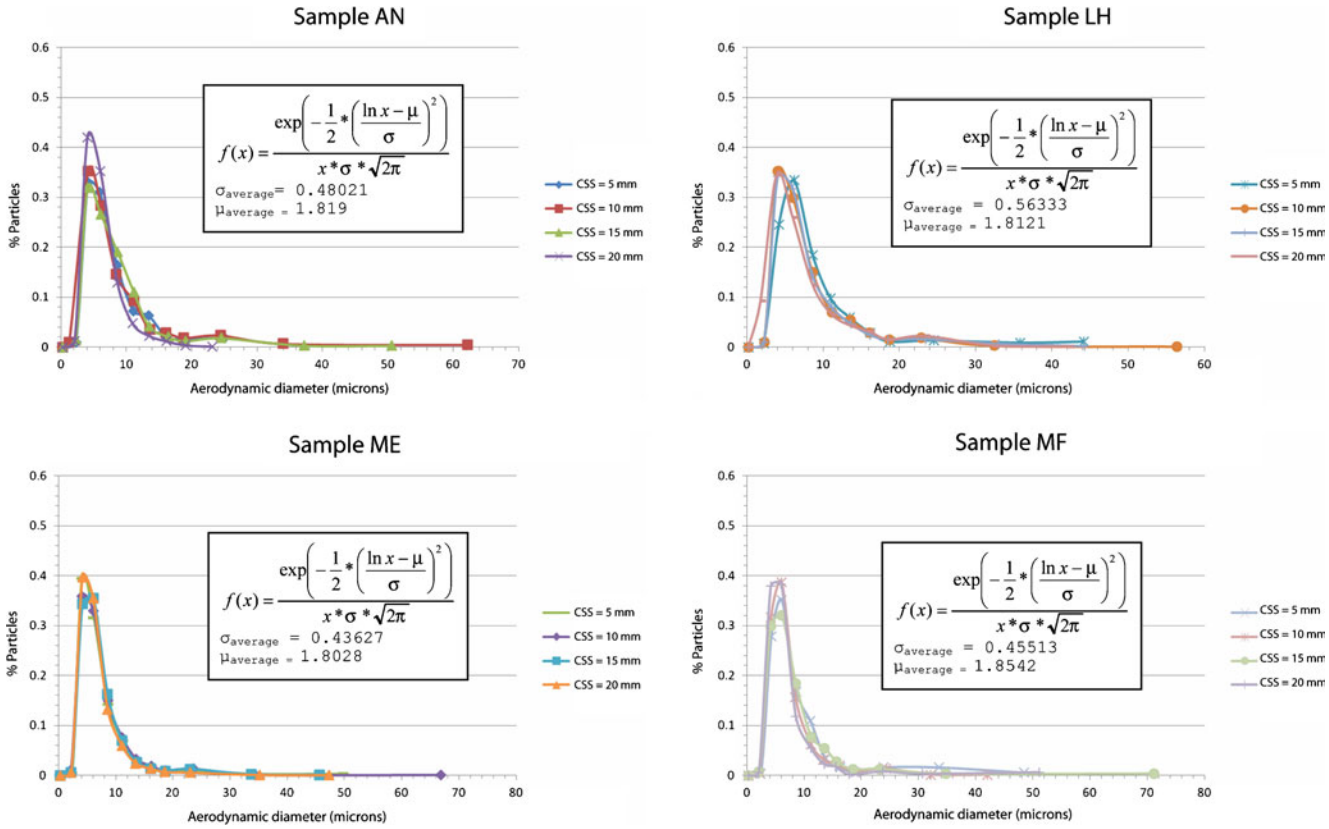

Fig. 12 Aerodynamic diameter distribution for airborne particles at aspiration rate of 1.5 l min^{-1}

environment. However, the morphological distribution of particles having size lower than 0.125 mm crushed product, independently from the jaw crusher aperture, can be used as an upper limit for the size and shape of the airborne

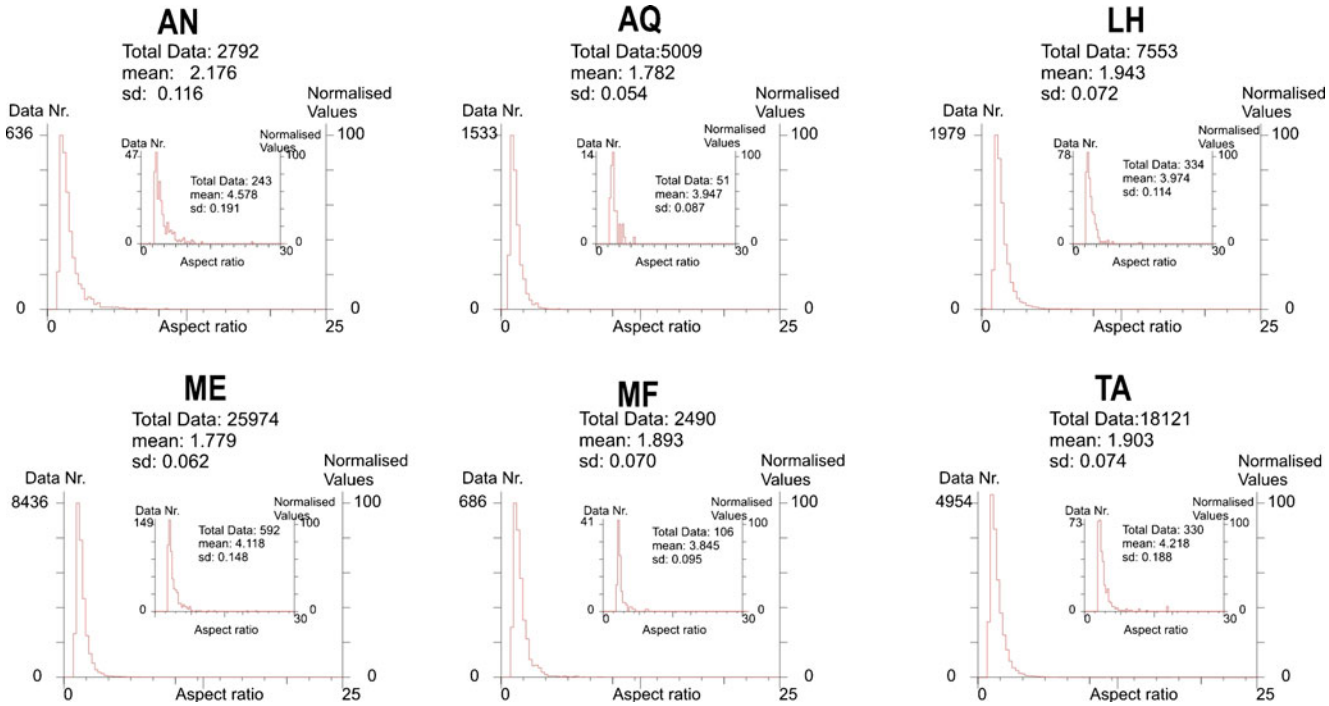

Fig. 13 Histograms for aspect ratio distribution of airborne particles. Small histograms refer to aspect ratio for filtered particles having fibre morphology

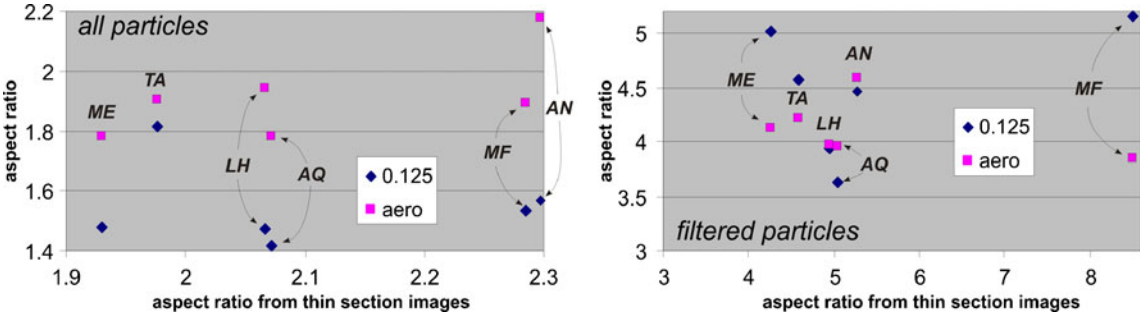

Fig. 14 Graphics correlating aspect ratio distribution deduced from rasterised images with aspect ratio distribution of particles from comminution (size lower than 0.125 mm) and airborne particles. Diagrams show that airborne particles systematically show a mean aspect ratio higher than the aspect ratio for the crushed particle (0.125 mm), for each sample. Conversely, this difference is scattered when the results are filtered for particles with fibrous morphology (right diagram). It is important to note that this distribution can be grouped selectively in function of the different petrographic properties of the original rocks

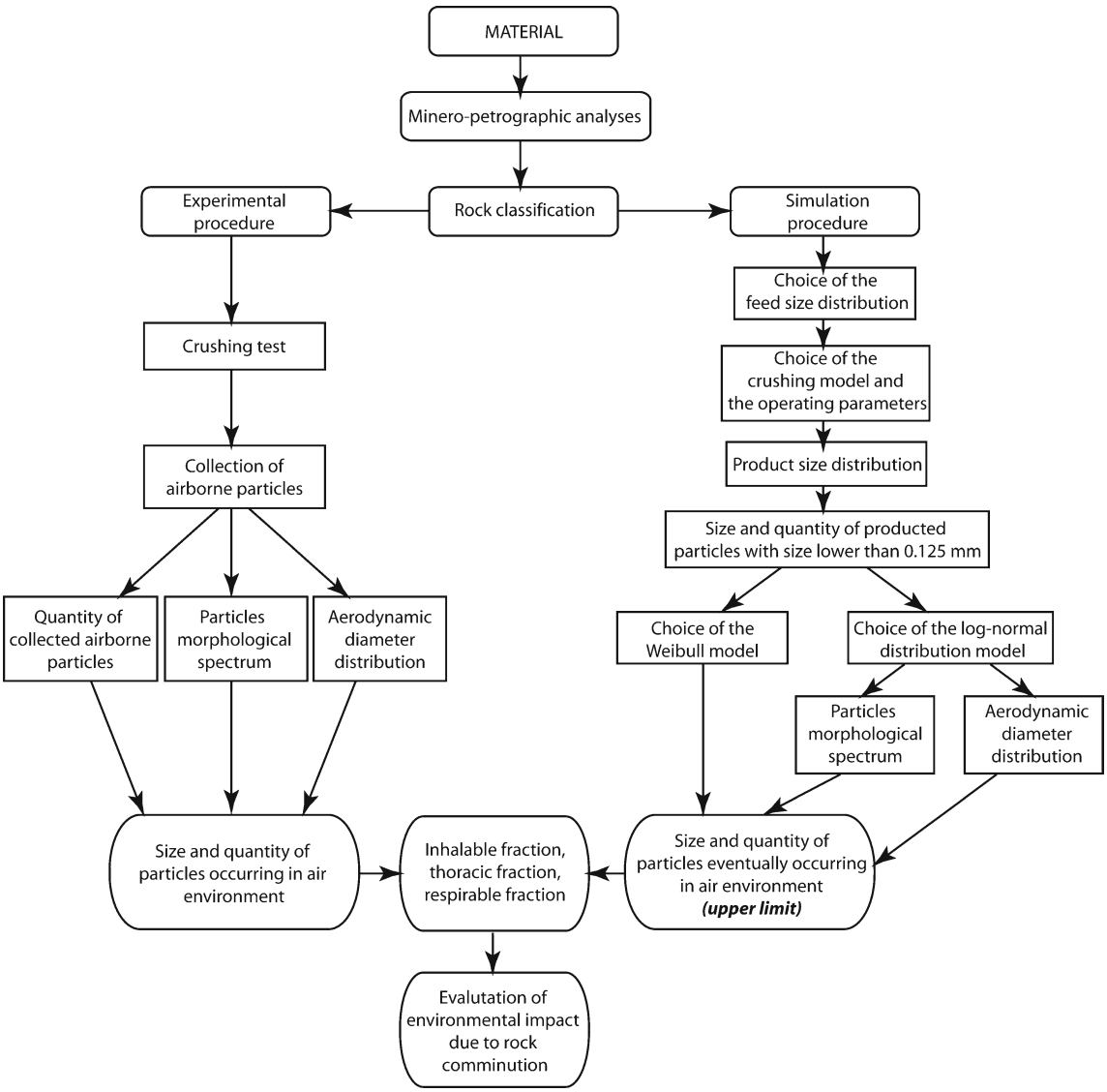

Fig. 15 Conceptual model proposing two procedures (experimental and simulation) for quantifying the size distribution and morphological characteristics of the particles produced by a comminution process and available in air environment

particles. Probably, comminution from the quaternary stone crushing can be used as an upper limit to primary, secondary and tertiary crushing.

The conceptual approach for the characterisation of the particles generated after comminution of a rock is shown in Fig. 15. We propose that, after the rock characterisation from the minero-petrographic and textural point of view, it is possible to consider two modus operandi, i.e. the experimental or the simulation procedure. If the texture properties of the material fall within those reported in this study, both ways are possible, otherwise the experimental procedure is obliged. In the experimental procedures it is sufficient to perform a crusher test for obtaining the comminution model and for determining the quantity and size distribution of material with size lower than 0.125 mm. The morphological and the aerodynamic diameter distribution as upper limit of the airborne particles can be also established. In the simulation way, it is possible to associate the textural characteristics of the material to the model that can be adopted to simulate the results of the comminution process. Both procedures allow to quantify the size distribution and morphological characteristics of the particles produced by a comminution process and available in air environment. The upper limit of inhalable, thoracic and respirable fraction can be consequently determined.

Conclusions

Our experimental approach investigated the production of PM from stone crushing industry and has implications on the dust dispersion in the air environment.

Within the parameters controlling the PM, our results suggest that the size and morphology of particles generated after rock comminution are linked to the rock properties in terms of petrographic textures. In particular, the occurrence of anisotropic structures (e.g. foliation) seems to enhance the generation of PM with fibrous morphology. If this is true, general implications on ophiolitic rocks involved in stone industry, such as the rocks tested in this work, can be addressed on the evaluation of the asbestos during abrasion.

Our results testify that the transfer of particles from crushed products to air environment is selective, as it operates in function of the size and the morphology of PM. The morphology and the aerodynamic distribution of airborne particles are independent both from the material (lithological class) tested in this work and the industrial operational parameters.

The application of mathematical models allows predicting the morphology and size range of airborne particles following the comminution processes, in order to develop predictive models able to quantify the dust dispersion in areas surrounding the source.

The environmental analyses and the normative regulation should consider information coming from the application of quantitative scientific studies.

Acknowledgements The authors are grateful to M. Serracino and M. Albano for the assistance at the electron microprobe and for SEM investigations. We thank the Editor (G. Lammel) for the revision management. Comments by an anonymous reviewer are highly acknowledged.

References

Belardi G, Desalvo F (2006) Simulation of the Realmonte (Sicily) mine comminution plant through a scaled-up process from laboratory tests. XXIII International Mineral Processing Congress 2:1695–1700

Breum NO (1999) The rotating drum dustiness tester: variability in dustiness in relation to sample mass, testing time, and surface adhesion. Ann Occup Hyg 43(8):557–566

Cattaneo A, Cavallo DM, Foà V (2006) Patologia umana conseguente all'inalazione di fibre di asbesto. Rend Soc Geol It 3:37–40

Chakravarti IM, Laha RC, Loy J (1967) Handbook of methods of applied statistics. Wiley, New York, 460 pp

Dahneke BA (1973) Slip correction factors for spherical bodies III: the form of general law. J Aerosol Sci 4:163–170

Dahneke BA, Cheng YS (1979) Properties of continuum source particle beams. I. Calculation methods and results. J Aerosol Sci 10:257–274

DeCarlo PF, Slowik JG, Worsnop DR, Davidovits P, Jimenez JI (2004) Particle morphology and density characterization by combined mobility and aerodynamic diameter Measurements. Part 1. Theory. Aerosol Scì Technol 38:1185–1205

Doll R (1955) Mortality from lung cancer in asbestos workers. Br J Ind Med 12:81–86

Evans KM (2005) The environment: a revolution in attitudes. Thomson Gale, Detroit, 227 pp

Gunter ME, Belluso E, Mottana A (2007) Amphiboles: environmental and health concerns. Rev Mineral Geochem 67:453–516

Health and Safety Executive (1997) Dust: general principles of protection. Health and Safety Executive, Sudbury, p 44

Johnson DL, Leith D, Reis PC (1987) Drag on non-spherical, orthotropic aerosol particles. J Aerosol Sci 18:87–97

Jones T, Blackmore P, Leach M, Bérubé K, Sexton K, Richards R (2002) Characterisation of airborne particles collected within and proximal to an opencast coalmine: South Wales, N.K. Environ Monit Assess 75:293–312

King R P. (2001). Modelling & simulation of mineral processing system, Butterworth-Heinemann.

Kissell F. N. (2003) Handbook for dust control in Minino. NIOSH Publication No. 2003-147, Information Circular 9465.

Liu HY, Kou SQ, Lindqvist PA (2002) Numerical simulation of the fracture process in cutting heterogeneous brittle material. (Int J Numer Anal Meth Geomech 26:1253–1278

Naidoo, R., Robins, T., Seixas, N., 2002. Respiratory diseases among south african coalminers, Safety in Mines Research Advisory Committee, Final Project Report. University of Natal (SA) and University of Michigan (USA), SIMHEALTH 607.

Petavratzi E, Kingman S, Lowndes I (2005) Particulates from mining operations: a review of sources, effects and regulations. Miner Eng 18:1183–1199

Petavratzi E, Kingman SW, Lowndes IS (2007) Assessment of the dustiness and the dust liberation mechanisms of limestone quarry operations. Chem Eng Process 46:1412–1423

Reed W. R. (2005) Significant dust dispersion models for mining operations. NIOSH Publication No. 2005-138, Information Circular 9478.

Rey F, Boutin C, Viallat JR, Steinbauer J, Alessandroni P, Jutisz P, Di Giambattista D, Billon-Galland MA, Hereng P, Dumortier P, De Vuyst P (1994) Environmental asbestotic pleural plaques in northeast Corsica: correlation with airborne and pleural mineralogic analysis. Environ Health Perspect 102:251–252

Ross M, Nolan RP (2003) History of asbestos discovery and use and asbestos-related disease in context with the occurrence of asbestos within ophiolite complexes. Geol Soc Am (Special Paper) 373:447–470

Salvini, F., 2004. Daisy 4.1 The Structural Data Integrated System Analyzer. Available at. Software, University of Roma Tre, Roma. Available from http://host.uniroma3.it/progetti/fralab.

US-EPA, 2012. Emissions Factors & AP 42, Compilation of Air Pollutant Emission Factors. Available from http://www.epa.gov/ttn/chief/ap42/index.html.

Van Gosen BS (2007) The geology of asbestos in the United States and its practical applications. Environ Eng Geosci 13:55–68

Vignaroli G, Rossetti F, Belardi G, Billi A (2011) Linking rock fabric to fibrous mineralisation: a basic tool for the asbestos hazard. Natural Hazards and Earth Science Systems 11:1267–1280

Whiten W.J., Walter G.W., White M.E. (1973) A breakage function suitable for crusher models. In: 4th Tewksbury Symposium, Melbourne, 19, pp 1–32

Whiten WJ (1972) A model for simulating crushing plants. J S Afr Inst Min Metall 72(10):257

Whiten, W.J. (1973) The simulation of crushing plants with models developed using multiple spline regression. In: Proceedings Application of Computer Methods in the Mineral Industry, 10th International Symposium, South African Institute of Mining and Metallurgy, Johannesburg, pp 317–323

Whiten, W.J., White, M.E. (1979) Modelling and simulation of high tonnage crushing plants. In: 12th International Mineral Processing Congress, Sao Paulo, Brazil, 2, pp 148-158

Wise DU, Funiciello R, Parotto M, Salvini F (1985) Topographic lineament swarms: clues to their origin from domain analysis of Italy. Geol Soc Am Bull 96:952–967

World Health Organization (1986) Asbestos and other natural mineral fibres, Environmental Health Criteria, No. 53, Geneva

World Health Organization (1999) Hazard Prevention and Control in the Work Environment: Airborne Dust, WHO/SDE/OEH/99.14

Zakrzewska AM, Capone PP, Iannò A, Tarzia V, Campopiano A, Villella E, Giardino R (2008) Calabrian ophiolites: dispersion of airborne asbestos fibers during mining and milling operations. Per Mineral 72:27–34